

# Bending loss of elliptical-hole core circular-hole holey fibers bent in arbitrary bending directions

著者	EGUCHI Masashi, TSUJI Yasuhide
journal or publication title	Applied Optics
volume	49
number	32
page range	6207-6212
year	2010
URL	<a href="http://hdl.handle.net/10258/00010163">http://hdl.handle.net/10258/00010163</a>

doi: info:doi/10.1364/AO.49.006207

# Bending loss of elliptical-hole core circular-hole holey fibers bent in arbitrary bending directions

Masashi Eguchi

*Department of Photonics System Technology, Chitose Institute of Science and  
Technology, Chitose, 066-8655 JAPAN*

*megu@ieee.org*

Yasuhide Tsuji

*Department of Electric and Electronic Engineering, Kitami Institute of Technology,  
Kitami, 090-8507 JAPAN*

*tsujiya@mail.kitami-it.ac.jp*

A holey fiber having a core with an elliptical-hole lattice structure, which is referred to as an elliptical-hole core circular-hole holey fiber (EC-CHF), can be easily designed as a single-polarization fiber by using the fundamental-space filling modes of the core and cladding lattices. However, since the guided mode in an EC-CHF has a polarization that arises from large geometrical anisotropy of the core lattice, the influence of the bending direction on the bending loss is a crucial issue for the practical implementation of EC-CHFs. Here, the bending losses of an EC-CHF bent in arbitrary angular orientations with respect to the core cross section are calculated numerically using the equivalent anisotropic step-index circular fiber model for a real EC-CHF and the influence of the bending direction of the fiber on the bending loss is discussed. © 2010 Optical Society of America

*OCIS codes:* 060.2310, 060.2400, 060.2420.

## 1. Introduction

Coherent optical fiber transmission systems can dramatically improve the receiver sensitivity compared with that of intensity-modulation/direct-detection systems and allow us to use phase or frequency modulation [1]. Polarization-state stabilization of two degenerate orthogonally polarized fundamental modes in a single mode fiber is required for the application of optical fibers to coherent lightwave systems. Imperfections in actually produced fibers and/or random perturbations arising from practical installations cause the degenerate fundamental modes to be nondegenerate, and thus can lead to polarization instability owing to mode coupling. Breaking axial symmetry of fiber cross sections is effective to stabilize the polarization state and various birefringent or single-polarization fibers using geometrical or stress effects have been proposed [2, 3]. Single-polarization fibers supporting only one polarization state are especially attractive for coherent optical fiber transmission systems because of a high resistance to external perturbations. Several single-polarization fibers based on a standard core-cladding structure have been proposed [4–9]. In addition, since holey fibers (HFs) with a high refractive-index contrast possess high controllability for their transmission characteristics, various single-polarization HFs have also been reported [10–12] and we have recently been proposed a novel one using the anisotropic fundamental-space filling mode (FSM) [13] of an elliptical-hole lattice [13, 14]. This HF is referred to as an elliptical-hole core circular-hole HF (EC-CHF), which is a

circular-hole HF having a core region with an elliptical-hole lattice structure, and shown in Fig. 1. The EC-CHF has not been fabricated so far. However, it may be fabricated by applying a manufacturing technique [15] that was used to fabricate a HF having a tiny elliptical hole in its solid core region. The radiation loss caused by the bend may be a worrisome issue for the practical implementation because the core region of the EC-CHF consists of air holes.

Theoretical evaluations of the bending losses of optical fibers have been reported so far. A standard bending loss formula derived by Marcuse is well known for the bending loss evaluation of standard round fibers [16] and has been applied to HFs by applying an effective-index method to the air-hole lattice region [14, 17–20]. If a fiber is bent uniformly with a constant radius, the bent fiber can be replaced by a straight fiber with an equivalent refractive index distribution [21] based on a conformal transformation [22] or be described in a cylindrical coordinate system [23]. Then, an alternative approach based on a 2D complex eigenmode analysis can be applied directly to real HF structures and is more faithful to the air-hole lattice structure than the approximated approach using the standard bending loss formula for circular fibers based on the effective-index method. Early in 2000, research efforts have been devoted to elucidate the bending properties of standard HFs having a solid core, which is formed by a single air-hole defect region, and a finite air-hole lattice cladding [24–27]. Although EC-CHFs whose core is also formed by an air-hole lattice consisting of elliptical holes have a more complicated structure than standard HFs, various

approaches have been recently applied for their bending loss evaluations [23]. However, the bending loss simulations in [23] are limited to the bend only in the direction of one of two axes of elliptical holes. On the other hand, since, in addition to having strong anisotropy in the core region, the EC-CHFs are a single-polarization fiber, a polarization conversion might arise from bending them and, thus, might raise the bending losses somewhat. Therefore, the dependence of the fiber angular orientation on the radiation losses (referred to as loss anisotropy) caused by bending is a crucial issue for the practical implementation of EC-CHFs and needs to be assessed in detail. It has already been indicated in [24,25] that the bending direction of bent HFs affects the bending losses also in standard HFs. However, the core regions of such standard HFs are made of an isotropic material and, thus, the loss anisotropy on the fiber bend arises from the configuration of a finite hexagonal lattice of air holes in the cladding. On the other hand, since EC-CHFs have strong anisotropy in the core itself, in EC-CHFs the core region will most strongly affect the loss anisotropy on the fiber bend. In this paper, by assuming an infinite uniform lattice cladding, we investigate how the anisotropy of the core region affects the loss anisotropy on the fiber bend of EC-CHFs.

The numerical analysis of the bending losses of EC-CHFs requires huge computations due to the discretization of the cross sections, because the EC-CHFs have a complicated core cross section. On the other hand, we have demonstrated that an equivalent step-index (SI) circular fiber model, in which the core region of an EC-CHF formed by an elliptical-hole lattice is approximated by a homogeneous medium

having the equivalent index of the elliptical-hole lattice, is valid for the bending loss evaluation, when the air-hole sizes are relatively small [23]. Thus, the bending losses of EC-CHFs are calculated numerically here by using the equivalent anisotropic SI circular fibers for real EC-CHFs, referred to as an equivalent anisotropic SI circular fiber model. The numerical approach for the bending loss evaluation of HFs using the equivalent anisotropic SI circular fiber model is first provided in Sections 2 and 3. The bending losses of EC-CHFs bent in arbitrary bending directions are discussed in Section 4.

## **2. Evaluation of the bending losses of HFs**

The numerical analysis of the bending losses of EC-CHFs generally has much more difficulty than that of standard optical fibers, because in EC-CHFs not only the cladding region but also the core region consists of an air-hole lattice. We recently demonstrated that when the relative FSM index difference [23] between the core and cladding regions is relatively small, the agreement among the approximate approach using the standard bending loss formula for circular fibers based on the effective-index method and the direct numerical approaches for real EC-CHF structures using a 2D vector finite-element method (V-FEM) and a 3D finite-element beam propagation method is fairly good through a comparison of the results obtained from various approaches for calculating the bending losses of EC-CHFs [23]. Figure 2 demonstrates the bending loss of a three-ring  $y$ EC-CHF bent in the orientation perpendicular to

the polarization direction of the guided mode. The three-ring  $y$ EC-CHF, which has 37 elliptical holes in the core as shown in Fig. 1(c), has a lattice pitch  $\Lambda$ , a circular hole size  $d_C/\Lambda = 0.23$ , an elliptical hole size  $d_L/\Lambda = 0.4025$ , and an ellipticity  $d_L/d_S = 3.6$ , and its refractive index is assumed to be 1.444. The bending losses (solid lines) calculated by the approximate approach using the standard bending loss formula for circular fibers by regarding a three-ring  $y$ EC-CHF as two equivalent SI circular fibers having equivalent core radii  $a$  of  $m\Lambda$  and  $(m + 0.5)\Lambda$  are compared with that (open circles) for the real EC-CHF structure obtained by the 2D complex eigenmode analysis using a cylindrical coordinate system in Fig. 2.  $m$  represents the number of core air-hole rings and here  $m = 3$ . The bending loss of the equivalent SI circular fiber having a core radius of  $3.5\Lambda$  is similar to that of the real EC-CHF. Moreover, for  $\Lambda = 1\mu\text{m}$ , the effective core areas of the real three-ring  $y$ EC-CHF and the equivalent SI circular fiber having a core radius of  $3.5\mu\text{m}$  were  $76.9$  and  $75.2\mu\text{m}^2$ , respectively. Therefore, the bending losses of EC-CHFs bent in arbitrary bending directions are approximately predicted here by applying the 2D complex eigenmode analysis using the 2D V-FEM [23] to an equivalent anisotropic SI circular fiber having an anisotropic core and an isotropic cladding, which are approximated by media having the refractive indices equal to the FSM indices [23] of the elliptical-hole and circular-hole lattices, respectively.



### 3. Bending loss evaluation of EC-CHFs using the equivalent anisotropic SI circular fiber model

The relative permittivity tensor of the anisotropic core of the simulated equivalent anisotropic SI circular fiber is defined by

$$\varepsilon_{r,1} = \begin{bmatrix} \varepsilon_{XX,1} & 0 & 0 \\ 0 & \varepsilon_{YY,1} & 0 \\ 0 & 0 & \varepsilon_{YY,1} \end{bmatrix}, \quad (1)$$

$$\varepsilon_{XX,1} = (n_{\text{eff,E}}^x)^2, \quad (2)$$

$$\varepsilon_{YY,1} = (n_{\text{eff,E}}^y)^2, \quad (3)$$

where  $n_{\text{eff,E}}^x$  and  $n_{\text{eff,E}}^y$  are the anisotropic FSM indices in the core region formed by an elliptical-hole lattice. In the relative permittivity tensor given by Eq. (1), the  $z$  component of the diagonal tensor in the core region is assumed to be simply the  $y$  component corresponding to the  $y$ -polarized fundamental mode of the  $y$ EC-CHF. However, since this component cannot be clearly defined for equivalent SI circular fibers, it might be an arithmetic mean of the  $x$  and  $y$  components or a geometrical mean of them or an average index based on the area ratio of the air-holes and the solid region. However, in our simulations, there was no significant difference among the results obtained by using only the  $y$  component, the arithmetic and the geometrical means. The reason seems to be that the  $z$  component of the electric field,  $E_z$ , in EC-CHFs is significantly smaller than the transverse components,  $E_x$  and  $E_y$ . The

relative permittivity of the isotropic cladding is given by

$$\varepsilon_{r,2} = (n_{\text{eff,C}})^2, \quad (4)$$

where  $n_{\text{eff,C}}$  represents the FSM index of the air-hole lattice cladding.

#### 4. Results and Discussions

The bending loss of an EC-CHF bent in arbitrary bending directions has been calculated by rotating the equivalent anisotropic SI circular fiber as shown in Fig. 3. Figure 4 shows the bending losses in the 0 and 90 degree orientations corresponding to the bends in the directions along the minor and major axes of elliptical holes in the core, respectively, for a two- ( $a = 2.5\Lambda$ ), three- ( $a = 3.5\Lambda$ ), and four-ring ( $a = 4.5\Lambda$ )  $y$ EC-CHFs against bending radius  $R$ . The bending losses drastically reduce with an increase in the number of hole-rings in the core, because the light confinement gets stronger in the EC-CHFs with more hole-rings in the core. Moreover, we can confirm that the bending losses in the orientation ( $\delta = 0^\circ$ ) perpendicular to the polarization direction of the guided mode are relatively small compared with those along the polarization direction. Figures 5-7 demonstrate the loss anisotropies on the fiber bend of equivalent anisotropic SI circular fibers having  $a = 2.5\Lambda$ ,  $3.5\Lambda$ , and  $4.5\Lambda$  corresponding to a two-, three-, and four-ring  $y$ EC-CHFs, respectively, with a bending radius of 2.5 cm.  $\delta = 0^\circ$  and  $90^\circ$  correspond to fiber bends, respectively, in the  $x$  and  $y$  directions in Fig. 1. All the simulated EC-CHFs are designed to operate as a single-polarization fiber and the guided mode is only a mode polarized along the major

axis of elliptical-holes in the core, which is the orientation of  $\varepsilon_{YY,1}$  in Fig. 3. We can see that, as well as Fig. 4, the minimum bending loss for every EC-CHF is obtained in the orientation ( $\delta = 0^\circ$ ) perpendicular to the polarization direction of the guided mode and toward the orientation along the polarization direction the bending loss increases smoothly. And it reaches its maximum at the orientation ( $\delta = 90^\circ$ ) along the polarization direction. This is because a bent waveguide can be regarded as an equivalent straight waveguide with a cross-sectional index distribution that increases toward the outside of the bend [23] and has a graded-index core profile that reaches its maximum at the edge of the core on the outside of the bend, and the equivalent core width decreases in the direction of the bend. Therefore, when the electric-field is polarized parallel to the direction of the bend ( $\delta = 90^\circ$ ), the bending loss is strongly influenced by the reduction of the equivalent core width and reaches its maximum. Moreover, the relative loss deviations in the bending direction were 31.8, 100.9, and 340.1 %, respectively, for the two-, three-, and four-ring EC-CHFs. Here, the relative loss deviation is defined by

$$\frac{\alpha_B(\delta = 90^\circ) - \alpha_B(\delta = 0^\circ)}{\alpha_B(\delta = 0^\circ)} \times 100. \quad (5)$$

We found that the relative loss deviation increases with the number of hole-rings in the core, because the bending loss gets smaller for EC-CHFs with more hole-rings in the core and, thus, changes more sensitively for the bending direction.

The mode field distribution in an equivalent anisotropic SI circular fiber ( $a = 3.5\Lambda$ )

for a  $\delta = 0^\circ$  bent three-ring  $y$ EC-CHF with  $R = 1\text{cm}$  is shown in Fig. 8. A significant radiation field is observed toward the outside of the bend and most of the radiation occurs in the direction of the bend. In addition, as seen from Fig. 8(b), the field displacement toward the outside of the bend is seen also in the core.

In this paper, to predict the loss anisotropy on the fiber bend of EC-CHFs, the bending losses of equivalent anisotropic SI circular fibers for the real EC-CHFs have been analyzed. However, the results obtained here will be available also to predict the bending loss properties of ordinary anisotropic SI fibers having an anisotropic circular core.

## 5. Conclusion

The bending losses of EC-CHFs having an elliptical-hole lattice core bent in arbitrary bending directions have been calculated numerically by regarding the real EC-CHF structures as equivalent anisotropic SI circular fibers. We confirmed that, in EC-CHFs, the minimum bending loss is obtained in the orientation perpendicular to the polarization direction of the guided mode and toward the orientation along the polarization direction the bending loss increases smoothly. In addition, we observed that the relative loss deviation depending on the bending direction drastically increases with the number of hole-rings in the core and most of the radiation arising from the bend occurs in the direction of the bend.

## References

1. G. P. Agrawal, *Fiber-Optic Communication Systems 3rd edition* (Wiley-Interscience, 2002).
2. D.N. Payne, A.J. Barlow, and J.J.R. Hansen, "Development of low- and high-birefringence optical fibers ," IEEE J. Quantum Electron. **QE-18**, 477-488 (1982).
3. J. Noda, K. Okamoto, and Y. Sasaki, "Polarization-maintaining fibers and their applications ," J. Lightwave Technol. **LT-4**, 1071-1089 (1986).
4. J.R. Simpson, R.H. Stolen, F.M. Sears, W. Pleibel, J.B. MacChesney, and R.E. Howard, "A single-polarization fiber ," J. Lightwave Technol. **LT-1**, 370-374 (1983).
5. A.W. Snyder and F. Rühl, "New single-mode single-polarisation fibre ," IEE Electron. Lett. **19**, 185-186 (1983).
6. M.P. Varnham, D.N. Payne, R.D. Birch, and E.J. Tarbox, "Single-polarisation operation of highly birefringent bow-tie optical fibres ," IEE Electron. Lett. **19**, 246-247 (1983).
7. T. Okoshi, T. Aihara, K. Kikuchi, "Prediction of the ultimate performance of side-tunnel single-polarisation fibre ," IEE Electron. Lett. **19**, 1080-1082 (1983).
8. K. Tajima, M. Ohashi, and Y. Sasaki, "A new single-polarization optical fiber ," J. Lightwave Technol. **7**, 1499-1503 (1989).
9. M.J. Messerly, J.R. Onstott, and R.C. Mikkelson, "A broad-band single polariza-

- tion optical fiber ,” J. Lightwave Technol. **9**, 817-820 (1991).
10. H. Kubota, S. Kawanishi, S. Koyanagi, M. Tanaka, and S. Yamaguchi, “Absolutely single polarization photonic crystal fiber ,” IEEE Photon. Technol. Lett. **16**, 182-184 (2004).
  11. J.R. Folkenberg, M.D. Nielsen, and C. Jakobsen, “Broadband single-polarization photonic crystal fiber ,” Opt. Lett. **30**, 1446-1448 (2005).
  12. T. Schreiber, F. Röser, O. Schmidt, J. Limpert, R. Iliew, F. Lederer, A. Petersson, C. Jacobsen, K.P. Hansen, J. Broeng, and A. Tünnermann, “Stress-induced single-polarization single-transverse mode photonic crystal fiber with low nonlinearity ,” Opt. Express **13**, 7621-7630 (2005).
  13. M. Eguchi and Y. Tsuji, “Single-mode single-polarization holey fiber using anisotropic fundamental space-filling mode ,” Opt. Lett. **32**, 2112-2114 (2007).
  14. M. Eguchi and Y. Tsuji, “Design of single-polarization elliptical-hole core circular-hole holey fibers with zero dispersion at  $1.55 \mu\text{m}$  ,” J. Opt. Soc. Am. B **25**, 1690-1701 (2008).
  15. W. Belardi, G. Bouwmans, L. Provino, and M. Douay, “Form-induced birefringence in elliptical hollow photonic crystal fiber with large mode area ,” IEEE J. Quantum Electron. **41**, 1558 -1564 (2005).
  16. D. Marcuse, “Curvature loss formula for optical fibers ,” J. Opt. Soc. Am. **66**, 216-220 (1976).

17. T.A. Birks, J.C. Knight, and P.St.J. Russell, "Endlessly single-mode photonic crystal fiber ," *Opt. Lett.* **22**, 961-963 (1997).
18. T. Sørensen, J. Broeng, A. Bjarklev, T.P. Hansen, E. Knudsen, S.E.B. Libori, H.R. Simonsen, and J.R. Jensen, "Spectral macro-bending loss considerations for photonic crystal fibres ," *IEE Proc. Optoelectron.* **149**, 206-210 (2002).
19. M.D. Nielsen, N.A. Mortensen, M. Albertsen, J.R. Folkenberg, A. Bjarklev, and D. Bonacinni, "Predicting macrobending loss for large-mode area photonic crystal fibers ," *Opt. Express* **12**, 1775-1779 (2004).
20. S. Février, R. Jamier, J.-M. Blondy, S.L. Semjonov, M.E. Likhachev, M.M. Bubnov, E.M. Dianov, V.F. Khopin, M.Y. Salganskii, and A.N. Guryanov, "Low-loss singlemode large mode area all-silica photonic bandgap fiber ," *Opt. Express* **14**, 562-569 (2006).
21. D. Marcuse, "Influence of curvature on the losses of doubly clad fibers ," *Appl. Opt.* **21**, 4208-4213 (1982).
22. M. Heiblum and J.H. Harris, "Analysis of curved optical waveguides by conformal transformation ," *IEEE J. Quantum. Electron.* **QE-11**, 75-83 (1975).
23. M. Eguchi and Y. Tsuji, "Bending loss evaluations of holey fibers having a core consisting of an elliptical-hole lattice by various approaches ," *IEEE J. Quantum Electron.* **46**, 601-609 (2010).
24. J. Olszewski, M. Szpulak, and W. Urbańczyk, "Effect of coupling between funda-

- mental and cladding modes on bending losses in photonic crystal fibers ,” *Opt. Express* **13**, 6015-6022 (2005).
25. T. Martynkien, J. Olszewski, M. Szpulak, G. Golojuch, W. Urbanczyk, T. Nasilowski, F. Berghmans, and H. Thienpont “Experimental investigations of bending loss oscillations in large mode area photonic crystal fibers ,” *Opt. Express* **15**, 13547-13556 (2007).
26. J. Olszewski, M. Szpulak, T. Martynkien, W. Urbańczyk, F. Berghmans, T. Nasilowski, and H. Thienpont, “Analytical evaluation of bending loss oscillations in photonic crystal fibers ,” *Opt. Commun.* **269**, 261-270 (2007).
27. N.H. Vu, I.-K. Hwang, and Y.-H. Lee, “Bending loss analyses of photonic crystal fibers based on the finite-difference time-domain method ,” *Opt. Lett.* **33**, 119-121 (2008).



## List of figures

Fig. 1 (Color online) A schematic of elliptical-hole core circular-hole holey fiber ( $y$ EC-CHF). (b) Two-ring  $y$ EC-CHF. (c) Three-ring  $y$ EC-CHF. (d) Four-ring  $y$ EC-CHF.

Fig. 2 Bending loss evaluations for a single-polarization three-ring  $y$ EC-CHF (open circles) bent in the orientation perpendicular to the polarization direction of the guided mode and two equivalent SI circular fibers (solid lines).

Fig. 3 (Color online) Bending of an equivalent anisotropic SI circular fiber in arbitrary bending directions.

Fig. 4 Estimation of the bending losses for the directions along the major and minor axes of elliptical holes in the core.

Fig. 5 Estimation of the bending loss ( $R = 2.5$  cm) of an equivalent anisotropic SI circular fiber ( $a = 2.5\Lambda$ ) for a two-ring  $y$ EC-CHF in arbitrary bending directions.

Fig. 6 Estimation of the bending loss ( $R = 2.5$  cm) of an equivalent anisotropic SI circular fiber ( $a = 3.5\Lambda$ ) for a three-ring  $y$ EC-CHF in arbitrary bending directions.

Fig. 7 Estimation of the bending loss ( $R = 2.5$  cm) of an equivalent anisotropic SI circular fiber ( $a = 4.5\Lambda$ ) for a four-ring  $y$ EC-CHF in arbitrary bending directions.

Fig. 8 (a) Mode field in an equivalent anisotropic SI circular fiber ( $a = 3.5\Lambda$ ) for a  $\delta = 0^\circ$  bent three-ring  $y$ EC-CHF with  $R = 1$ cm. (b) Zoom around the core region.

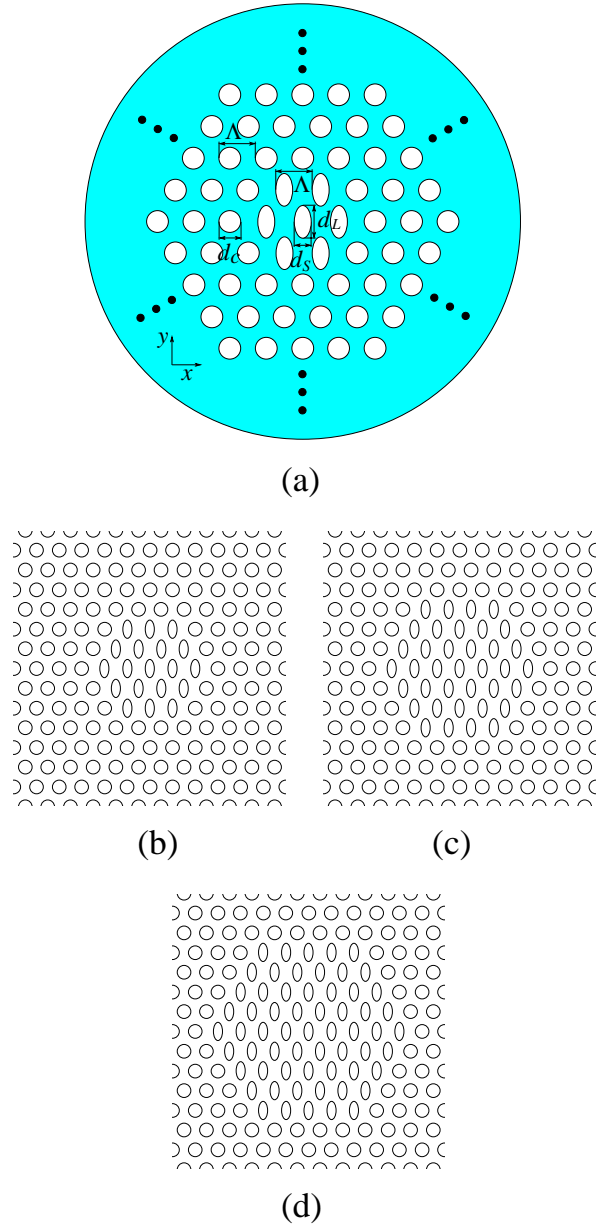


Fig. 1. (Color online) A schematic of elliptical-hole core circular-hole holey fiber ( $y$ EC-CHF). (b) Two-ring  $y$ EC-CHF. (c) Three-ring  $y$ EC-CHF. (d) Four-ring  $y$ EC-CHF.

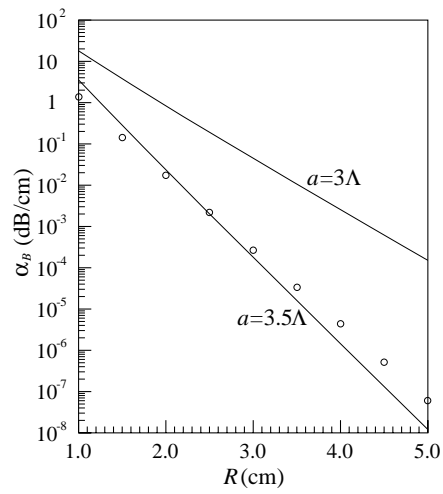


Fig. 2. Bending loss evaluations for a single-polarization three-ring  $y$ EC-CHF (open circles) bent in the orientation perpendicular to the polarization direction of the guided mode and two equivalent SI circular fibers (solid lines).

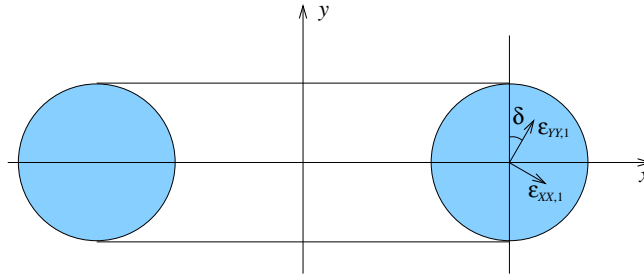


Fig. 3. (Color online) Bending of an equivalent anisotropic SI circular fiber in arbitrary bending directions.

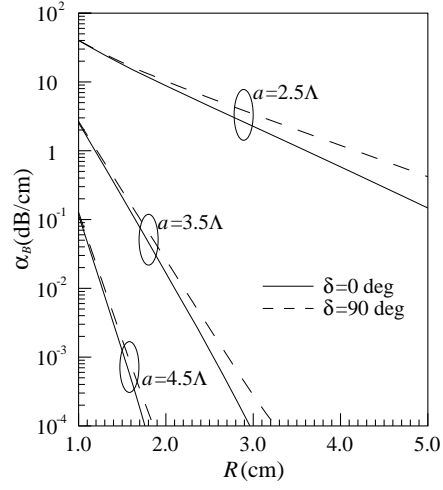


Fig. 4. Estimation of the bending losses for the directions along the major and minor axes of elliptical holes in the core.

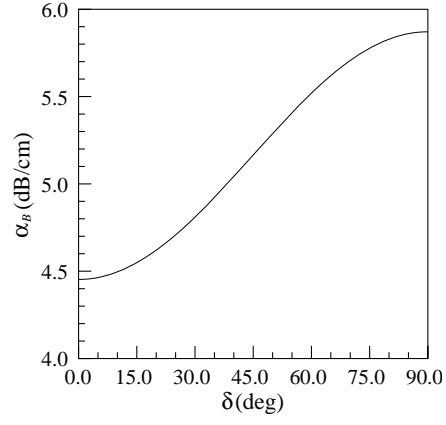


Fig. 5. Estimation of the bending loss ( $R = 2.5$  cm) of an equivalent anisotropic SI circular fiber ( $a = 2.5\Lambda$ ) for a two-ring  $y$ EC-CHF in arbitrary bending directions.

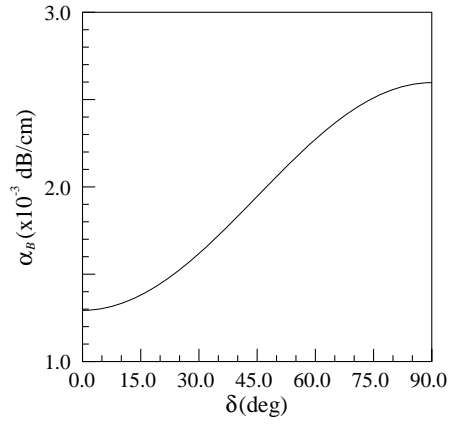


Fig. 6. Estimation of the bending loss ( $R = 2.5$  cm) of an equivalent anisotropic SI circular fiber ( $a = 3.5\lambda$ ) for a three-ring  $y$ EC-CHF in arbitrary bending directions.

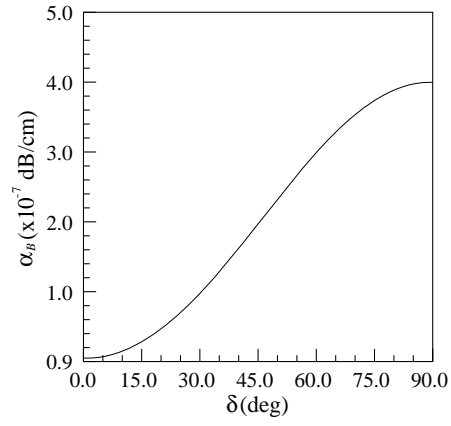
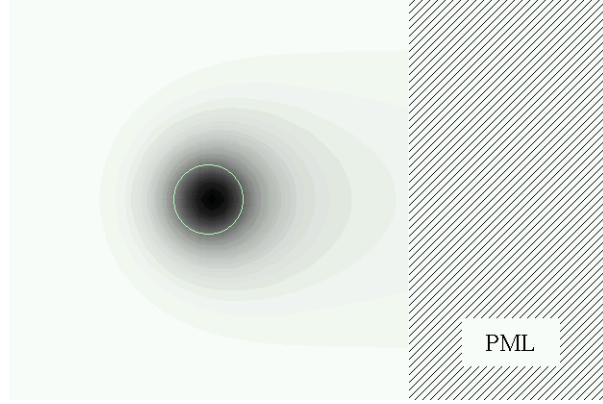
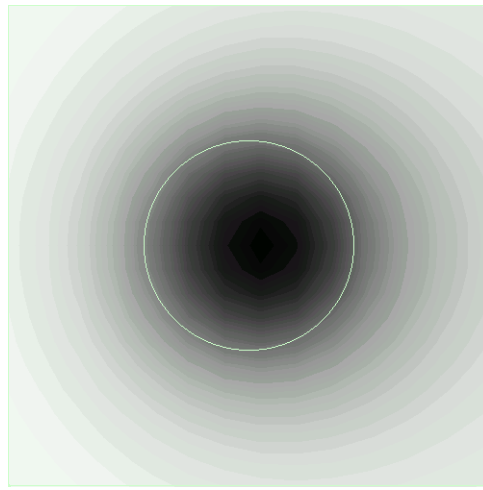


Fig. 7. Estimation of the bending loss ( $R = 2.5$  cm) of an equivalent anisotropic SI circular fiber ( $a = 4.5\lambda$ ) for a four-ring  $y$ EC-CHF in arbitrary bending directions.





(a)



(b)

Fig. 8. (a) Mode field in an equivalent anisotropic SI circular fiber ( $a = 3.5\Lambda$ ) for a  $\delta = 0^\circ$  bent three-ring  $y$ EC-CHF with  $R = 1\text{cm}$ . (b) Zoom around the core region.